THE JOURNAL OF BIOLOGICAL CHEMISTRY VOL. 287, NO. 50, pp. 42389–42399, December 7, 2012

Metabolic Mechanism of Mannan in a Ruminal Bacterium, *Ruminococcus albus*, Involving Two Mannoside Phosphorylases and Cellobiose 2-Epimerase

DISCOVERY OF A NEW CARBOHYDRATE PHOSPHORYLASE, β-1,4-MANNOOLIGOSACCHARIDE PHOSPHORYLASE[*S]

Received for publication, June 12, 2012, and in revised form, October 19, 2012 Published, JBC Papers in Press, October 23, 2012, DOI 10.1074/jbc.M112.390336

Ryosuke Kawahara[1], **Wataru Saburi**[1,2], **Rei Odaka, Hidenori Taguchi, Shigeaki Ito, Haruhide Mori, and Hirokazu Matsui**

From the Research Faculty of Agriculture, Hokkaido University, N-9, W-9, Sapporo 060-8589, Japan

Background: Characteristics of two 4-*O*-β-D-mannosyl-D-glucose phosphorylases from *Ruminococcus albus* were investigated.
Results: One enzyme was specific for 4-*O*-β-D-mannosyl-D-glucose, as observed for the *Bacteroides fragilis* enzyme, but the other showed high activity toward mannooligosaccharides longer than β-1,4-mannobiose.
Conclusion: Two phosphorylases play distinct roles in the metabolism of mannan.
Significance: A new enzyme catalyzing the phosphorolysis of β-1,4-mannooligosaccharides was identified.

Ruminococcus albus **is a typical ruminal bacterium digesting cellulose and hemicellulose. Cellobiose 2-epimerase (CE; EC 5.1.3.11), which converts cellobiose to 4-*O*-β-D-glucosyl-D-mannose, is a particularly unique enzyme in *R. albus*, but its physiological function is unclear. Recently, a new metabolic pathway of mannan involving CE was postulated for another CE-producing bacterium, *Bacteroides fragilis*. In this pathway, β-1,4-mannobiose is epimerized to 4-*O*-β-D-mannosyl-D-glucose (Man-Glc) by CE, and Man-Glc is phosphorolyzed to α-D-mannosyl 1-phosphate (Man1*P*) and D-glucose by Man-Glc phosphorylase (MP; EC 2.4.1.281). *Ruminococcus albus* NE1 showed intracellular MP activity, and two MP isozymes, RaMP1 and RaMP2, were obtained from the cell-free extract. These enzymes were highly specific for the mannosyl residue at the non-reducing end of the substrate and catalyzed the phosphorolysis and synthesis of Man-Glc through a sequential Bi Bi mechanism. In a synthetic reaction, RaMP1 showed high activity only toward D-glucose and 6-deoxy-D-glucose in the presence of Man1*P*, whereas RaMP2 showed acceptor specificity significantly different from RaMP1. RaMP2 acted on D-glucose derivatives at the C2- and C3-positions, including deoxy- and deoxyfluoro-analogues and epimers, but not on those substituted at the C6-position. Furthermore, RaMP2 had high synthetic activity toward the following oligosaccharides: β-linked glucobioses, maltose, *N,N′*-diacetylchitobiose, and β-1,4-mannooligosaccharides. Particularly, β-1,4-mannooligosaccharides served as significantly better acceptor substrates for RaMP2 than D-glucose. In the phosphorolytic reactions, RaMP2 had weak activity toward β-1,4-mannobiose but efficiently degraded β-1,4-mannooligosaccharides longer than β-1,4-mannobiose. Consequently, RaMP2 is thought to catalyze the phosphorolysis of β-1,4-mannooligosaccharides longer than β-1,4-mannobiose to produce Man1*P* and β-1,4-mannobiose.**

Ruminococcus albus is a typical ruminal bacterium, producing various cellulolytic enzymes, including cellulase (EC 3.2.1.4) (1), β-glucosidase (EC 3.2.1.21) (2), and cellobiose phosphorylase (EC 2.4.1.20) (3). Cellobiose 2-epimerase (CE[3]; EC 5.1.3.11), which converts cellobiose to 4-*O*-β-D-glucosyl-D-mannose, is a unique enzyme acting on cellulose-related carbohydrates in *R. albus* (4), but the physiological meaning of its epimerization of cello-oligosaccharides is unclear.

Once the CE gene of *R. albus* NE1 was cloned (5), the CE genes were identified based on the amino acid sequence similarities in various bacteria, including a non-cellulolytic bacterium, *Bacteroides fragilis* NCTC9343 (6). In *B. fragilis*, the CE gene comprises the operon along with the genes encoding β-mannanase and 4-*O*-β-D-mannosyl-D-glucose phosphorylase (MP; EC 2.4.1.281), which specifically catalyzes the phosphorolysis of 4-*O*-β-D-mannosyl-D-glucose (Man-Glc) to α-D-mannosyl phosphate (Man1*P*) and D-glucose (7), implying that CE is involved in the metabolism of mannan, in which it converts β-1,4-mannobiose to Man-Glc for further phosphorolysis.

Known inverting carbohydrate phosphorylases catalyzing the phosphorolysis of a glycoside with anomeric inversion have catalytic domains that are structurally similar to inverting gly-

* This work was supported in part by Kakenhi, Grants-in-aid for Young Scientists (B) 24780091, of the Ministry of Education, Culture, Sports, Science, and Technology of Japan.
[S] This article contains supplemental Table S1 and Fig. S1.
[1] Both authors contributed equally to this work.
[2] To whom correspondence should be addressed: Research Faculty of Agriculture, Hokkaido University, N-9, W-9, Sapporo 060-8589, Japan. Tel./Fax: 81-11-706-2508; E-mail: saburiw@chem.agr.hokudai.ac.jp.

[3] The abbreviations used are: CE, cellobiose 2-epimerase; MP, 4-*O*-β-D-mannosyl-D-glucose phosphorylase; Man-Glc, 4-*O*-β-D-mannosyl-D-glucose; Man1*P*, α-D-mannosyl phosphate; GH, glycoside hydrolase; TLC, thin layer chromatography; DP, degree of polymerization; RaMP1, *R. albus* MP1 (Rumal_0852); RaMP2, *R. albus* MP2 (Rumal_0099); rRaMP1, recombinant RaMP1; rRaMP2, recombinant RaMP2.

TABLE 1
Primers used in this study
Single and double underlines indicate restriction sites for NdeI and XhoI, respectively.

Name	Sequence (5′ → 3′)	Orientation	Purpose
RaMP1 7 N	GATAAATATGAGTATTATCCGTTTCCATAG	Sense	Amplification of *RaMP1* gene
RaMP1 7 C	CTTTCACCTTAACAAAATAAAGAATCTATC	Antisense	Amplification of *RaMP1* gene
RaMP1 sen1	GGAACGTTTAGGTATAAACGCAGTATT	Sense	Sequence analysis
RaMP1nde	GAGCGACATATGATACACGAAAAATAC	Sense	Preparation of expression plasmid
RaMP1 xho nonhis	CAATGTAATCCTCGAGATATCAGATATC	Antisense	Preparation of expression plasmid
RaMP2 N	CTACCGAATGACCAAAAGCTG	Sense	Amplification of *RaMP2* gene
RaMP2 C3	GGTGAAAGATCAGATGCGAGTACG	Antisense	Amplification of *RaMP2* gene
RaMP2 nde	GGTGGAAATTCATATGAAGACACAG	Sense	Preparation of expression plasmid
RaMP2 xho nonhis	CTTTTCTCTTGATCTCGAGATATTATATC	Antisense	Preparation of expression plasmid
T7	TAATACGACTCACTATAGGG	Sense	Sequence analysis
T3	GCAGCAATTATAGCACAACGATG	Antisense	Sequence analysis
T7 terminator	GCTAGTTATTGCTCAGCGG	Antisense	Sequence analysis

coside hydrolases (8, 9). Thus, the inverting phosphorylases are classified into glycoside hydrolase (GH) families on the basis of the similarity of their amino acid sequences (10). Only limited information concerning MP from *B. fragilis* is available, but this enzyme was recently categorized into GH family 130 together with the putative proteins from the genome sequence of known bacterial species, the amino acid sequences of which are similar to that of *B. fragilis* MP. In this family, three-dimensional structures of *Thermotoga maritima* MSB8 TM1225 protein (Protein Data Bank code 1VKD), *Bacteroides thetaiotaomicron* VPI-5482 BT_4094 protein (Protein Data Bank code 3R67), and *Parabacteroides distansonis* ATCC 8503 BDI_3141 protein (Protein Data Bank code 3TAW) were elucidated, although their biochemical properties have not been examined thus far. These proteins are formed by five-bladed β-propeller folds, which are observed in the glycoside hydrolases belonging to GH families 32 (11, 12), 43 (13–18), and 68 (19, 20).

R. albus 7 has several putative β-1,4-mannanase genes and two MP-like genes (*Rumal_0099* and *Rumal_0852*) in the genome, indicating that this bacterium also has components necessary to metabolize mannan via epimerization and phosphorolysis, as observed in *B. fragilis*. *Rumal_0852* and *Rumal_0099* encode proteins with 59 and 27% sequence identity to *B. fragilis* MP, respectively. In this study, two MP isozymes from *R. albus* NE1, which is phylogenetically close to *R. albus* 7 (5), were characterized in detail, and the physiological functions of these enzymes in the metabolism of mannan are discussed.

EXPERIMENTAL PROCEDURES

Preparation of Man-Glc—For the enzyme assay, highly pure Man-Glc was prepared. A reaction mixture of 210 ml containing 100 mg/ml locust bean gum (Wako Pure Chemical Industries, Osaka, Japan), 1 unit/ml β-mannanase from *Aspergillus niger* (Shin Nihon Chemical, Anzyo, Japan), and 10 mM sodium acetate buffer (pH 4.0) was incubated at 37 °C for 24 h. The β-1,4-mannobiose produced was purified by carbon-celite column chromatography, as previously reported (21), and epimerized by CE as follows. A reaction mixture consisting of 50 mg/ml mannobiose, 0.1 unit/ml CE from *R. albus* NE1 (22), and 20 mM sodium phosphate buffer (pH 7.5) was incubated at 37 °C for 24 h. Man-Glc was purified, desalted, and freeze-dried, as described previously (21).

Identification of MP Isozymes in the Cell-free Extract of R. albus NE1—MP activity of the cell-free extract of *R. albus* NE1, obtained from 1.5 liters of the culture fluid (5), was detected by thin layer chromatography (TLC). Six μl of cell-free extract of *R. albus* NE1 was mixed with 2 μl of 100 mM Man-Glc and 2 μl of 50 mM reaction buffer (pH 7.0) and incubated at 37 °C for 3 h. Sodium phosphate buffer or MES-NaOH buffer was used as reaction buffer. The reaction mixture of 1 μl was analyzed by TLC, in which a developing solvent of acetonitrile/ethyl acetate/1-propanol/water (85:20:50:30, v/v/v/v) was used. The chromatogram was visualized by spraying a detection reagent (acetic acid/sulfuric acid/anisaldehyde, 100:2:1, v/v/v) and heating. The cell-free extract was subjected to DEAE-Sepharose CL-6B column chromatography (1.5 × 9.0 cm; GE Healthcare), in which adsorbed protein was eluted by a linear gradient of 0 – 0.5 M NaCl in 20 mM MES-NaOH buffer (pH 6.5). Enzyme activity was checked by TLC analysis as described above. Two active peaks (the enzymes eluted by high and low concentrations of NaCl were designated as RaMP1 and RaMP2, respectively) were further purified by butyl-Sepharose CL-6B (1.5 × 9.0 cm; GE Healthcare), hydroxyapatite (1.5 × 12 cm; Seikagaku, Tokyo), and Superdex 200 (1.6 × 60 cm; GE Healthcare) column chromatography. Finally, the sample was separated by SDS-PAGE. The masses of the tryptic peptides derived from the ~40-kDa protein were measured and assigned to the theoretical values for Rumal_0099 and Rumal_0852 proteins, as described elsewhere (23).

Production and Purification of Recombinant RaMP1 and RaMP2—The genomic DNA of *R. albus* NE1 as the template, Primestar HS DNA polymerase (Takara Bio, Otsu, Japan), and the primers listed in Table 1 were used in the PCR. The *RaMP1* and *RaMP2* genes were amplified by PCR and cloned into the EcoRV site of pBluescript II SK(+) vector (Stratagene, La Jolla, CA). The DNA sequences of the cloned genes were analyzed with the ABI Prism 310 genetic analyzer (Applied Biosystems, Foster City, CA). These plasmids were used as the templates in the PCR to construct the expression plasmids. NdeI and XhoI sites were introduced to the 5′ and 3′ termini of the target gene, respectively, by PCR (primers listed in Table 1) and cloned into the NdeI and XhoI sites of the pET-23a vector (Novagen, Darmstadt, Germany).

The transformants of *Escherichia coli* BL21 (DE3) harboring the expression plasmid of RaMP1 or RaMP2 were cultured in

0.5 and 1.5 liters of LB broth containing 100 μg/ml ampicillin, respectively, at 37 °C until the A_{600} reached 0.6. The protein production was induced by the addition of isopropyl β-D-thiogalactoside at a final concentration of 0.1 mM, and the incubation was continued at 18 °C for 16 h. The recombinant enzymes were purified from the *E. coli* cell extract. The concentrations of the purified enzymes were determined based on the concentration of each amino acid after acid hydrolysis (24).

Enzyme Assay—A reaction mixture of 50 μl consisting of the appropriate concentration of enzyme diluted with 20 mM MES-NaOH buffer (pH 6.5) containing 1 mg/ml bovine serum albumin, 100 mM sodium phosphate buffer (pH 6.5), and 2 mM Man-Glc was incubated at 37 °C for 10 min. The enzyme reaction was terminated by boiling the mixture for 3 min after the addition of 25 μl of 4 M Tris-HCl buffer (pH 7.0). The D-glucose produced was measured by the glucose oxidase-peroxidase method (25). One unit of enzyme activity was defined as the amount of enzyme producing 1 μmol of D-glucose in 1 min under these conditions.

To determine the optimum pH, the reaction buffer was changed to 100 mM sodium citrate buffer (pH 3.0–6.0), MES-NaOH buffer (pH 6.0–7.0), HEPES-NaOH buffer (pH 7.0–8.5), and glycine-NaOH buffer (pH 8.5–10.5). Sodium phosphate buffer (pH 6.5) was added as the substrate to the reaction mixture at the final concentration of 10 mM.

Temperature and pH stabilities were evaluated by the residual activity after temperature treatment (incubation at various temperatures for 20 min at pH 6.5) and pH treatment (incubation at various pH values for 24 h at 4 °C), respectively. The values over which the enzymes retained more than 90% of their original activities were considered to be stable ranges.

The kinetic parameters for phosphorolysis and synthesis of Man-Glc were calculated from the initial velocities toward various concentrations of Man-Glc and inorganic phosphate and of Man1*P* and D-glucose, respectively, by fitting to the equation for a sequential Bi Bi mechanism (26). Non-linear regression was performed with Grafit version 7.0.2 (Erithacus Software, West Sussex, UK).

Product inhibition analysis was carried out to determine the order of substrate binding and product release. First, the rate of phosphorolysis catalyzed by rRaMP1 and rRaMP2 toward Man-Glc in the presence of 0–2 mM Man1*P* was measured at varying concentrations of Man-Glc and 10 mM sodium phosphate buffer (pH 6.5) or at varying concentrations of sodium phosphate buffer (pH 6.5) and 2 mM Man-Glc. Then, in the case of rRaMP2, the phosphorolysis of Man-Glc was measured in the presence of 0–100 mM cellobiose at varying concentrations of Man-Glc and 10 mM sodium phosphate buffer (pH 6.5) or at varying concentrations of sodium phosphate buffer (pH 6.5) and 2 mM Man-Glc. In the case of rRaMP1, initial velocities for the synthesis of Man-Glc were measured in the presence of 0–20 mM Man-Glc at varying concentrations of Man1*P* and 50 mM D-glucose or at varying concentrations of D-glucose and 5 mM Man1*P*.

The rates for the synthesis of Man-Glc were measured as follows. A reaction mixture of 50 μl consisting of an appropriate concentration of enzyme, 50 mM MES-NaOH buffer (pH 6.5), 0.25–10 mM Man1*P* (sodium salt hydrate; Sigma), and 10–200 mM D-glucose (Wako Pure Chemical Industries) were incubated at 37 °C for 10 min and heated at 80 °C for 5 min. The released inorganic phosphate was measured following Lowry and Lopez (27). The apparent kinetic parameters for the synthetic reactions toward various acceptor substrates were determined by fitting the initial rates at various concentrations of acceptors in the presence of 10 mM Man1*P* to the Michaelis-Menten equation. The acceptor substrates tested were from the following suppliers: D-mannose, D-allose, 3-*O*-methyl-D-glucose, D-xylose, 1,5-anhydro-D-glucitol, methyl α-D-glucoside, and methyl β-D-glucoside were from Wako Pure Chemical Industries; 2-deoxy-D-glucose and D-glucosamine were from Tokyo Chemical Industry (Tokyo, Japan); 2-deoxy-2-fluoro-D-glucose, sophorose, and 6-deoxy-D-glucose were from Sigma; *N*-acetyl-D-glucosamine, maltose, cellobiose, and gentiobiose were from Nacalai Tesque (Kyoto, Japan); 3-deoxy-D-glucose, 3-deoxy-3-fluoro-D-glucose, and 6-deoxy-6-fluoro-D-glucose were from Carbosynth (Berkshire, UK); the series of mannooligosaccharides was from Megazyme; and *N*,*N*′-diacetyl chitobiose and laminaribiose were from Seikagaku.

The phosphorolytic velocity of rRaMP2 toward β-1,4-mannooligosaccharides was determined based on the amount of β-1,4-mannooligosaccharides with reduced chain length (D-mannose was measured in the reaction toward β-1,4-mannobiose) using HPLC. A reaction mixture of 200 μl consisting of an appropriate concentration of enzyme, 10 mM sodium phosphate buffer (pH 6.5), and various concentrations of β-1,4-mannooligosaccharides was incubated at 37 °C for 10 min and heated at 80 °C for 5 min. The reaction mixture was applied to HPLC under the following conditions: injection volume, 10 μl; column, Sugar D (4.6 × 250 mm; Nacalai Tesque); eluent, 65% acetonitrile; flow rate, 0.8 ml/min; detection, pulsed amperometry.

Analysis of Reaction Products toward β-1,4-Mannooligosaccharides by rRaMP2—Phosphorolytic activities of rRaMP2 toward β-1,4-mannotriose and β-1,4-mannotetraose were detected by TLC. A reaction mixture of 10 μl containing 0.24 μM rRaMP2, 20 mM β-1,4-mannotriose or β-1,4-mannotetraose, and 10 mM sodium phosphate buffer (pH 6.5) was incubated at 37 °C. One μl of the reaction mixture taken at 0, 30, 60, and 120 min was spotted on a TLC plate and dried immediately to stop the reaction. Developing solvent and detection conditions were as described above.

Structural Analysis of the Oligosaccharides Produced by the Synthetic Reaction—The oligosaccharides produced by recombinant RaMP1 (rRaMP1) were prepared as follows. A reaction mixture of 0.2 ml consisting of 493 nM rRaMP1, 50 mM MES-NaOH buffer (pH 6.5), 250 mM D-glucose or D-xylose, and 250 mM Man1*P* was incubated at 37 °C for 3 h. The reaction products were purified by HPLC as described previously (28). The synthetic reaction of recombinant RaMP2 (rRaMP2) was performed in a reaction mixture of 1 ml, consisting of 79 nM rRaMP2, 50 mM MES-NaOH buffer (pH 6.5), 100 mM Man1*P*, and 100 mM acceptor substrate. The reaction was carried out at 37 °C for 12 h. Cellobiose, β-1,4-mannobiose, and *N*,*N*′-diacetylchitobiose were used as acceptors. The reaction products were purified by gel filtration column chromatography under the following conditions: column, Bio-Gel P-2

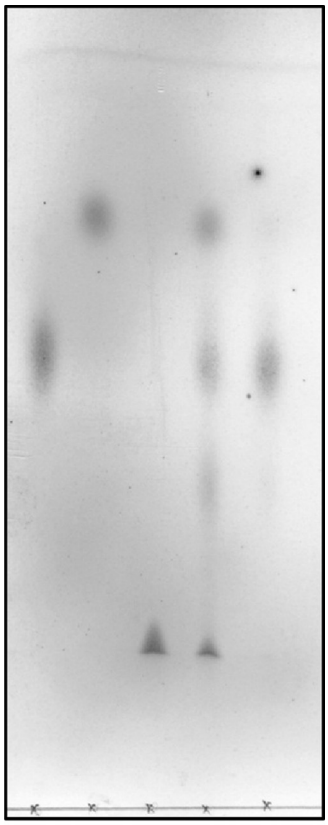

FIGURE 1. **Detection of MP activity in the cell-free extract of *R. albus* NE1.** Phosphorolytic activity of the cell-free extract of *R. albus* NE1 toward Man-Glc in the presence or absence of inorganic phosphate was analyzed by TLC. *S1*, Man-Glc; *S2*, glucose; *S3*, Man1*P*. Man-Glc was degraded only in sodium phosphate buffer.

(1.8 × 100 cm; Bio-Rad); eluent, water; flow rate, 2.5 ml/h; fraction volume, 3 ml.

Electrospray ionization-MS of the oligosaccharides produced was carried out using an Exactive mass spectrometer (Thermo Scientific, San Jose, CA). The samples were introduced by flow injection. Methanol was used as a mobile phase solvent. The positive ion was detected under the following conditions: spray voltage, 3.00 kV; capillary temperature, 300 °C. Nuclear magnetic resonance (NMR) spectra were recorded in D_2O (Wako Pure Chemical Industries) at 300 K using an ECP-400 (400 MHz; Jeol, Tokyo, Japan). Sodium 3-(trimethylsilyl)-1-propanesulfonate was used as the standard. A series of two-dimensional homo- and heteronuclear correlated spectra (COSY, HSQC, HSQC-TOCSY, and HMBC) were obtained.

RESULTS

Identification of RaMP1 and RaMP2 in the Cell-free Extract of R. albus NE1—MP activity in the cell-free extract of *R. albus* NE1 was analyzed by TLC (Fig. 1). Man-Glc was degraded to D-glucose and Man1*P* only in the presence of inorganic phosphate, indicating that *R. albus* NE1 produces intracellular MP. *R. albus* MP was purified to identify the gene encoding it. MP activity was identified in two peaks, RaMP1 and RaMP2, eluted by high and low concentrations of NaCl, respectively, via anion exchange column chromatography using a DEAE-Sepharose CL-6B column (data not shown). Two MPs were further purified, and the masses of the tryptic peptides were analyzed by matrix-assisted laser desorption ionization time-of-flight mass spectrometry (supplemental Fig. S1). The obtained masses of the digests of RaMP1 and RaMP2 matched with the theoretical values of the proteins encoded by *Rumal_0852* and *Rumal_0099* from *R. albus* 7, respectively. The analyzed tryptic fragments derived from RaMP1 and RaMP2 covered 27 and 36% of their entire sequences, respectively.

Production, Purification, and General Properties of Recombinant RaMP1 and RaMP2—The genes encoding RaMP1 and RaMP2 were obtained from the genomic DNA of *R. albus* NE1 by PCR. The sequences of the amplified genes were completely identical to the corresponding genes of *R. albus* 7. These genes were overexpressed in *E. coli*, and the recombinant enzymes were purified to homogeneity. From 0.5 and 1.5 liters of the culture broths of the *E. coli* transformants, 6.8 and 11.4 mg of the purified rRaMP1 and rRaMP2 (the specific activities were 55.2 and 2.03 units/mg) were obtained. RaMP1 and RaMP2 were 45 and 38 kDa on SDS-PAGE, respectively (data not shown), which coincided well with the theoretical masses from their amino acid sequences, but were 80 and 209 kDa on a gel filtration column, respectively. These results indicate that RaMP1 and RaMP2 exist as a homodimer and homohexamer in solution, respectively. Both RaMP1 and RaMP2 showed highest activity at pH 6.5, and their optimum temperatures were 50 and 45 °C, respectively. RaMP1 retained original activity in a pH range of 4.5–10.5 and below 45 °C, whereas RaMP2 was stable at pH 3.5–9.5 and below 40 °C.

Kinetic Mechanisms for Phosphorolysis and Synthesis of Man-Glc by RaMP1 and RaMP2—Initial reaction velocities for phosphorolysis at various concentrations of Man-Glc and inorganic phosphate were measured to investigate the kinetic mechanisms of RaMP1 and RaMP2. The lines obtained for both enzymes from double reciprocal plots of $1/v$ *versus* 1/[Man-Glc] at various concentrations of inorganic phosphate were linear and crossed at a certain point (Fig. 2). This indicates that these enzymes catalyze the phosphorolysis of Man-Glc through a sequential Bi Bi mechanism involving the formation of a ternary complex. To investigate the orders of substrate binding and product release, product inhibition analysis was carried out (Fig. 3). Man1*P* acted as a competitive inhibitor of rRaMP1 and rRaMP2 against both Man-Glc and inorganic phosphate, as observed for several cellobiose phosphorylases (3, 29), indicating that these substrates bind to the enzymes in random order, and Man1*P* can be the second product (the first substrate in the reverse reaction). Therefore, a possible kinetic mechanism for these enzymes is a random order Bi Bi mechanism or a random-ordered Bi Bi mechanism (3, 29). In the reverse reaction of rRaMP1, Man-Glc served as a competitive inhibitor against both Man1*P* and D-glucose, indicating that rRaMP1 catalyzes phosphorolysis of Man-Glc through a random order Bi Bi mechanism. In the case of rRaMP2, inhibition of phosphorolysis toward Man-Glc by cellobiose, which is not phosphorolyzed by rRaMP2 but acts as an acceptor substrate of this enzyme (described below), was analyzed, because a very high concentration of Man-Glc is required for the inhibition analysis of the synthetic reaction. Uncompetitive inhibition by cellobiose was

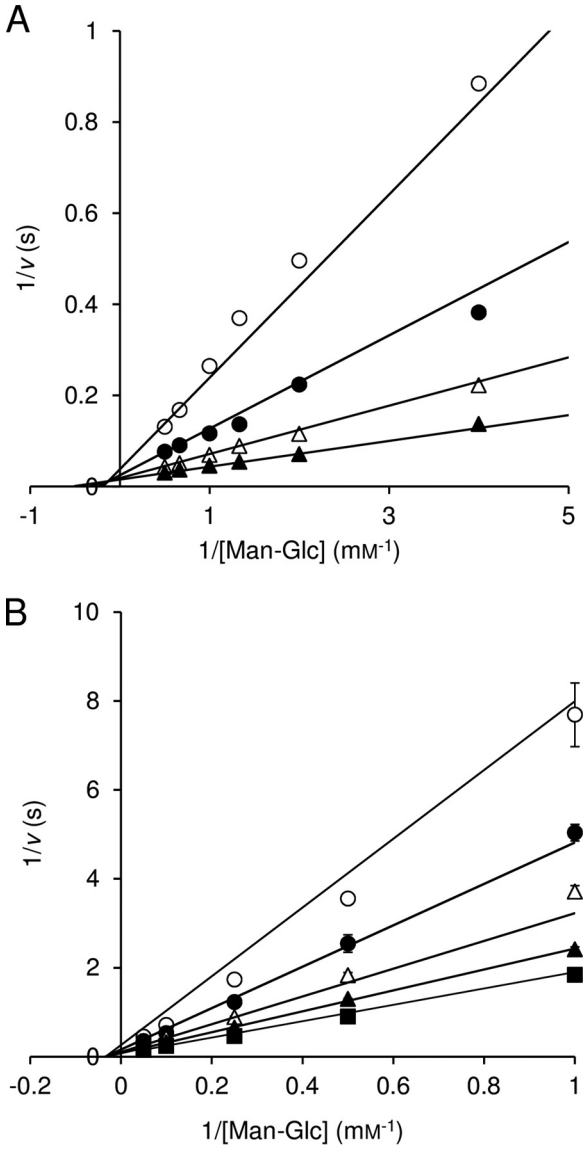

FIGURE 2. **Double reciprocal plot for the phosphorolysis of Man-Glc by rRaMP1 and rRaMP2.** The initial velocities for phosphorolysis of Man-Glc at various concentrations of Man-Glc and inorganic phosphate were measured. *A*, rRaMP1. Concentrations of inorganic phosphate were 2.5 mM (*open circles*), 5.0 mM (*filled circles*), 10 mM (*open triangles*), and 20 mM (*filled triangles*). *B*, rRaMP2. Concentrations of inorganic phosphate were 0.125 mM (*open circles*), 0.25 mM (*filled circles*), 0.5 mM (*open triangles*), 1 mM (*filled triangle*), and 3 mM (*filled squares*). Data are the mean ± S.D. (*error bars*) for three independent experiments.

observed when the concentration of inorganic phosphate was varied, presumably because of the formation of an enzyme-phosphate-cellobiose complex, which does not react or reacts very slowly. On the other hand, cellobiose competitively inhibited the phosphorolysis of Man-Glc at various concentrations of Man-Glc. This inhibition occurred by binding of cellobiose to +1 and +2 subsites or to −1 and +1 subsites. The former case indicates that D-glucose (cellobiose) also can be the second product, and the kinetic mechanism of the phosphorolysis of Man-Glc by rRaMP2 is a random order Bi Bi mechanism as rRaMP1. The possibility of the latter case makes the order of release (binding) of Man1*P* and D-glucose (cellobiose) ambiguous. However, in the kinetic analysis of the synthetic reaction toward cellobiose and Man1*P*, no substrate inhibition by cellobiose was observed, indicating that cellobiose acts only as an acceptor substrate and does not bind to −1 and +1 subsites. The kinetic parameters for the phosphorolysis and synthesis of Man-Glc are summarized in Table 2. In the phosphorolytic reaction of Man-Glc, rRaMP1 had a 4.8-fold higher k_{cat} and 91-fold lower $K_{m(MG)}$ compared with rRaMP2. The $K_{m(P_i)}$ of rRaMP2 was considerably lower (12-fold) than that of rRaMP1.

Kinetic parameters for the synthesis of Man-Glc with rRaMP1 and rRaMP2 were determined from the initial reaction rates for various concentrations of Man1*P* and D-glucose (Table 2). rRaMP1 had a 6.6-fold higher k_{cat} value for the synthetic reaction than rRaMP2, as it did for the phosphorolytic reaction. The $K_{m(Glc)}$ value of rRaMP1 was 3.7-fold lower than that of rRaMP2, indicating that the +1 subsite of RaMP1 is more suitable for binding the D-glucose moiety than RaMP2, consistent with the higher affinity of rRaMP1 toward Man-Glc than that of rRaMP2. The rRaMP2 $K_{m(Man1P)}$ value was 18-fold lower than that of rRaMP1, corresponding with the observation that RaMP2 has higher affinity toward inorganic phosphate than RaMP1 during the phosphorolysis of Man-Glc.

The internal consistency of the kinetic parameters of rRaMP1 and rRaMP2 was confirmed with the Haldane relationship for a sequential Bi Bi mechanism ($K = (k_{cat}{}^{P}K_{s(Man1P)}K_{mGlc})/(k_{cat}{}^{s}K_{sMan\text{-}Glc}K_{m(P_i)})$, where $k_{cat}{}^{P}$ and $k_{cat}{}^{s}$ represent k_{cat} for phosphorolytic and synthetic reactions, respectively) (30). Values of 0.435 ± 0.062 and 0.658 ± 0.137 were obtained for *K* of rRaMP1 and rRaMP2, respectively, from the kinetic parameters in Table 2. These values were similar in magnitude to the value 0.272 ± 0.021 experimentally obtained with rRaMP1 at pH 6.5 at 37 °C for the thermodynamic equilibrium constant (*K*) calculated from the following equation,

$$K = ([\text{Man1}P][\text{Glc}])/([\text{Man-Glc}][\text{phosphate}]) \quad \text{(Eq. 1)}$$

Substrate Specificity of RaMP1 and RaMP2 in Phosphorolytic Reactions—D-Glucose was not detected in the reaction carried out in the presence of rRaMP1 or rRaMP2 and cellobiose or lactose even at a 10-fold higher enzyme concentration than used for the enzyme assay toward Man-Glc, indicating that these enzymes are highly specific to the mannosyl residue at the non-reducing end of the substrate.

Acceptor Specificity of RaMP1 in Synthetic Reaction—The acceptor specificity of rRaMP1 was investigated based on the initial reaction rates toward Man1*P* and various acceptor substrates. rRaMP1 showed a very narrow acceptor specificity. Almost all the oligosaccharides tested were not recognized as acceptor substrates. Only laminaribiose served as a poor acceptor substrate for rRaMP1. The apparent kinetic parameters, $k_{cat(app)}$ and $K_{m(app)}$, for laminaribiose, determined in the presence of 10 mM Man1*P*, were 7.6-fold lower and 6.0-fold higher than those for D-glucose, respectively (Table 3).

rRaMP1 was not active toward D-glucose derivatives with changes at the C2-position, and it was less active toward derivatives with changes at the C3-position compared with D-glucose. The monodeoxygenation at the 6-OH-position was less effective for RaMP1 than at the other positions. The $k_{cat(app)}$ and $K_{m(app)}$ values of rRaMP1 for 6-deoxy-D-glucose were 1.4-

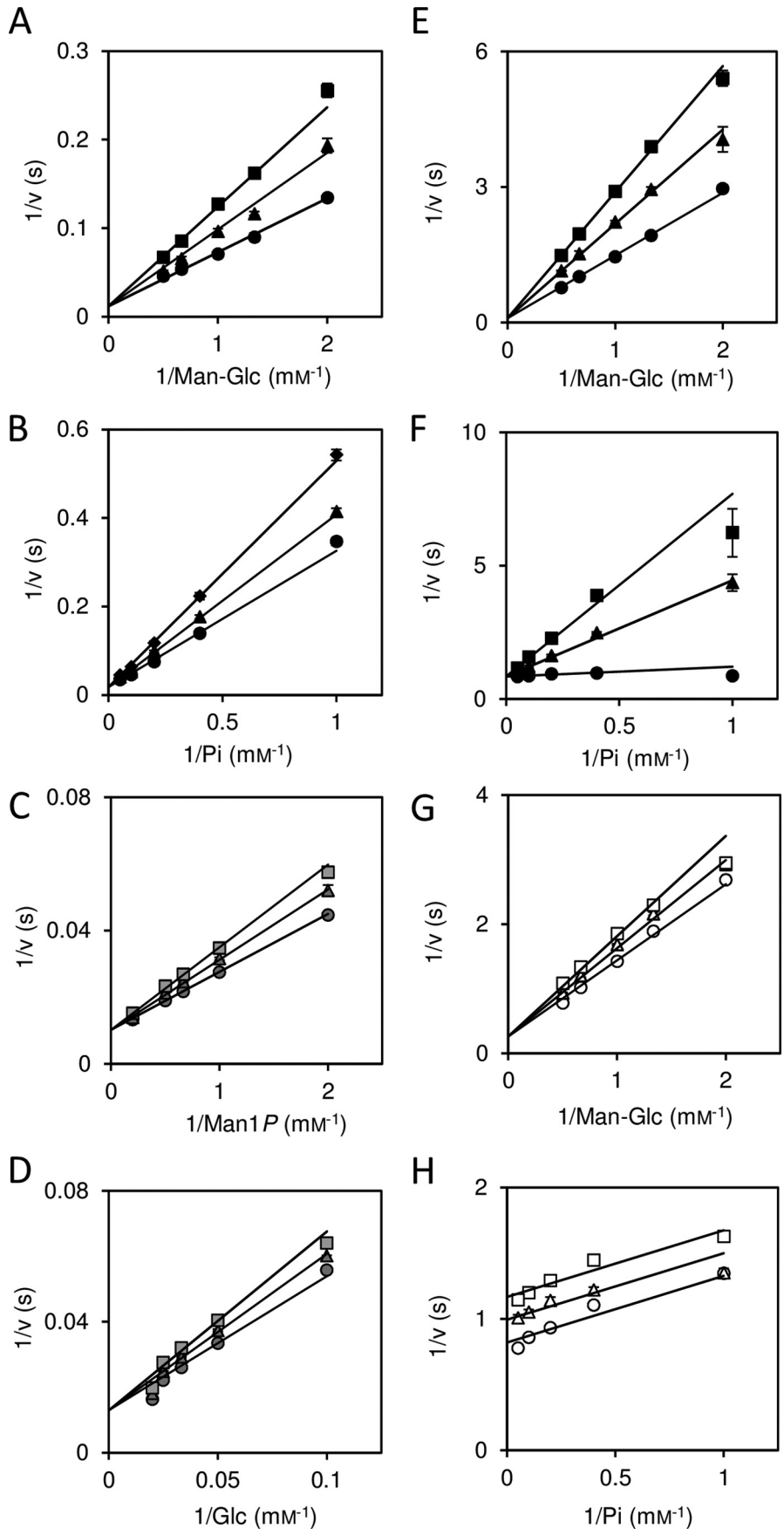
A
1/v (s)
1/Man-Glc (mM-1)
B
1/v (s)
1/Pi (mM-1)
C
1/v (s)
1/Man1P (mM-1)
D
1/v (s)
1/Glc (mM-1)
E
1/v (s)
1/Man-Glc (mM-1)
F
1/v (s)
1/Pi (mM-1)
G
1/v (s)
1/Man-Glc (mM-1)
H
1/v (s)
1/Pi (mM-1)

TABLE 2

Kinetic parameters for the phosphorolysis and synthesis of Man-Glc by rRaMP1 and rRaMP2

Substrate concentrations were as follows: phosphorolysis of rRaMP1, 0.25–2.0 mM Man-Glc and 2.5–20 mM inorganic phosphate; synthesis of rRaMP1, 0.5–5.0 mM Man1*P* and 10–50 mM D-glucose; phosphorolysis of rRaMP2, 1.0–20 mM Man-Glc and 0.125–3.0 mM inorganic phosphate; synthesis of rRaMP2, 0.25–2.0 mM Man1*P* and 25–200 mM D-glucose. ND, not determined.

	rRaMP1	rRaMP2
Phosphorolysis		
k_{cat} (s^{-1})(mM)	83.3 ± 5.8	17.5 ± 1.3
K_m(Man-Glc) (mM)	0.304 ± 0.070	27.7 ± 2.7
K_m(Pi) (mM)	5.34 ± 0.47	0.444 ± 0.108
K_s(Man-Glc) (mM)	7.70 ± 0.24	30.3 ± 6.0
K_s(Pi)(mM)[a]	135	ND
Synthesis		
k_{cat} (s^{-1})	204 ± 20	30.9 ± 1.9
K_m(Glc) (mM)	38.2 ± 5.2	142 ± 12
K_m(Man1*P*) (mM)	5.80 ± 0.93	0.324 ± 0.097
K_s(Glc) (mM)	7.65 ± 1.45	51.5 ± 25.7
K_s(Man1*P*) (mM)	1.16	ND

[a] Values were calculated from the relationships of kinetic parameters, $K_s(\text{Man-Glc})K_m(P_i) = K_s(P_i)K_m(\text{Man-Glc})$.

and 4.6-fold higher than those for D-glucose, respectively. On the other hand, 6-deoxy-6-fluoro-D-glucose and D-xylose were considerably less favorable acceptor substrates than 6-deoxy-D-glucose. This enzyme had a 3.3-fold lower $k_{cat(app)}$ and 6.0-fold higher $K_{m(app)}$ for 6-deoxy-6-fluoro-D-glucose than those for D-glucose, and a saturation curve was not obtained for D-xylose because of its very high $K_{m(app)}$. These results indicate that the 6-OH partially contributes to the enzyme-substrate interaction as a hydrogen bond donor and that the methylene group of D-glucose is also involved in stabilization of the transition state, presumably through the hydrophobic interaction.

Structures of oligosaccharides produced by the synthetic reaction of rRaMP1 with D-glucose and D-xylose as acceptors were investigated. A single oligosaccharide was produced in each reaction, and 2.0 and 4.9 mg of product was obtained by HPLC, respectively. The structures of these oligosaccharides were elucidated by electrospray ionization-MS and NMR. The oligosaccharides produced from the reactions with D-glucose and D-xylose gave signals at 365.11 and 335.09 m/z $[M + Na]^+$, respectively. Each oligosaccharide had a correlation peak between the 4C of the acceptor and the 1H of the D-mannosyl residue at the non-reducing end. The $^1J_{CH}$ values for the D-mannosyl residues at the non-reducing ends of these oligosaccharides in ^{13}C NMR (insensitive nuclei enhanced by polarization transfer) were 161 Hz, indicating that D-mannosyl residues were bound to the acceptor substrates through a β-linkage (31). On the basis of these results, the oligosaccharides produced in the synthetic reactions in the presence of D-glucose and D-xylose were identified as Man-Glc and 4-*O*-β-D-mannosyl-D-xylose, respectively. The chemical shifts of ^1H and ^{13}C NMR analyses are summarized in supplemental Table S1.

Acceptor Specificity of RaMP2 in Synthetic Reaction—rRaMP2 was not active when D-glucose was derivatized at the C6-position but showed very broad acceptor specificity (Table 3). rRaMP2 showed the highest $k_{cat(app)}/K_{m(app)}$ toward *N*-acetyl-D-glucosamine among the 2-OH derivatives of D-glucose, although *N*-acetyl-D-glucosamine has a bulky acetamide group at the C2-position. All of the D-glucose derivatives with changes at the C3-position acted as acceptor substrates of rRaMP2. The $k_{cat(app)}$ and $K_{m(app)}$ values for these derivatives were considerably lower than for D-glucose. The $K_{m(app)}$ value for 3-deoxy-D-glucose was too low to determine the value.

rRaMP2 had $k_{cat(app)}/K_{m(app)}$ values for 1,5-anhydro-D-glucitol and methyl α-D-glucoside similar to that for D-glucose, and the $k_{cat(app)}/K_{m(app)}$ for methyl β-D-glucoside was 2.1-fold higher than for D-glucose. All of the oligosaccharides acted as acceptor substrates of rRaMP2. The $k_{cat(app)}/K_{m(app)}$ values for β-linked glucobioses were 1.4–4.5-fold higher than for D-glucose due to low $K_{m(app)}$ values for these oligosaccharides. Cellobiose was the best acceptor substrate for rRaMP2 among the β-linked glucobioses in terms of its $k_{cat(app)}/K_{m(app)}$ value, followed by gentiobiose. rRaMP2 also had a 3.4-fold lower $K_{m(app)}$ for *N*,*N*′-diacetylchitobiose. The $k_{cat(app)}/K_{m(app)}$ for maltose was 50% of that for D-glucose; thus, the acceptor site of rRaMP1 efficiently accommodates even an α-linked oligosaccharide. D-Mannose was a poor acceptor substrate of rRaMP2 compared with D-glucose, but rRaMP2 showed 7.3–20-fold higher $k_{cat(app)}/K_{m(app)}$ values for β-1,4-mannooligosaccharides than for D-glucose. The $k_{cat(app)}/K_{m(app)}$ values for β-1,4-mannooligosaccharides increased depending on the degree of polymerization (DP) up to β-1,4-mannotetraose, whereas those for substrates longer than β-1,4-mannotetraose slightly decreased with increasing substrate chain length, although a lower $K_{m(app)}$ was observed for longer β-1,4-mannooligosaccharides.

Structural analysis of oligosaccharides produced in the synthetic reactions of rRaMP2 toward cellobiose, β-1,4-mannobiose, and *N*,*N*′-diacetylchitobiose was performed. In contrast to rRaMP1, rRaMP2 produced several oligosaccharides with different DPs. The resulting reaction mixtures were subjected to gel filtration column chromatography (data not shown). The yields of the oligosaccharides purified were as follows: from cellobiose, DP3, 9.5 mg; DP4, 2.7 mg; DP5, 0.8 mg; and DP6, 0.4 mg; from β-1,4-mannobiose, DP3, 4.5 mg; DP4, 2.8 mg; DP5, 0.8 mg; and DP6, 0.3 mg; from *N*,*N*′-diacetylchitobiose, DP3, 2.4 mg; DP4, 1.3 mg; DP5, 0.8 mg; and DP6, 0.6 mg. Molecular masses of the obtained oligosaccharides were analyzed by electrospray ionization-MS. The masses were as follows: the products from cellobiose, 527.16, 689.26, 851.27, and 1013.32 m/z $[M + Na]^+$; from β-1,4-mannobiose, 527.16, 689.21, 851.27, and 1013.32 m/z $[M + Na]^+$; from *N*,*N*′-diacetylchitobiose,

FIGURE 3. **Product inhibition analyses of rRaMP1 and rRaMP2.** Product inhibition analyses of rRaMP1 and rRaMP2 are shown in *A–D* and *E–H*, respectively. *A* and *B* (*E* and *F* for rRaMP2), inhibition of the phosphorolysis of Man-Glc by Man1*P* against Man-Glc and inorganic phosphate, respectively. *C* and *D*, inhibition of the synthesis of Man-Glc by Man-Glc against Man1*P* and D-glucose, respectively. *G* and *H*, inhibition of the phosphorolysis of Man-Glc by cellobiose against Man-Glc and inorganic phosphate, respectively. *Black circles*, *triangles*, *squares*, and *diamonds*, 0, 1, 2, and 2.5 mM, respectively. *Gray circles*, *triangles*, and *squares*, 0, 10, and 20 mM, respectively. *Open circles*, *triangles*, and *squares*, 0, 50, and 100 mM, respectively. Data are the mean ± S.D. (*error bars*) for three independent experiments.

TABLE 3

Apparent kinetic parameters for the synthetic reaction of rRaMP1 and rRaMP2

Kinetic parameters were calculated by fitting the initial velocities toward various concentrations of acceptor substrates in the presence of 10 mM Man1*P* to the Michaelis-Menten equation. Only k_{cat}/K_m values are provided when saturation curves were not obtained due to high K_m values (estimated to be higher than 200 mM). Data are mean ± S.D. for three independent experiments. ND, not determined.

	rRaMP1			rRaMP2		
	$k_{cat(app)}$	$K_{m(app)}$	$k_{cat}/K_{m(app)}$	$k_{cat(app)}$	$K_{m(app)}$	$k_{cat}/K_{m(app)}$
	s^{-1}	mM	s^{-1} mM^{-1}	s^{-1}	mM	s^{-1} mM^{-1}
D-Glucose	126 ± 1	25.9 ± 0.1	4.86	34.5 ± 0.2	172 ± 5	0.201
2-Deoxy-D-glucose	ND	ND	ND	11.7 ± 0.8	90.7 ± 8.0	0.129
2-Deoxy-2-fluoro-D-glucose	ND	ND	ND	5.71 ± 0.16	48.7 ± 1.8	0.117
D-Mannose	ND	ND	ND	5.12 ± 0.05	45.6 ± 0.3	0.112
N-Acetyl-D-glucosamine	ND	ND	ND	15.8 ± 1.7	107 ± 13	0.148
3-Deoxy-D-glucose	ND	ND	ND	0.412 ± 0.002[a]	< 0.05[b]	ND
3-Deoxy-3-fluoro-D-glucose	ND	ND	0.0526	0.940 ± 0.015	6.44 ± 0.68	0.146
D-Allose	ND	ND	ND	0.667 ± 0.018	6.14 ± 0.71	0.109
3-*O*-Methyl-D-glucose	ND	ND	0.0764	0.763 ± 0.010	7.82 ± 0.34	0.0976
6-Deoxy-D-glucose	177 ± 21	119 ± 18	1.49	ND	ND	ND
6-Deoxy-6-fluoro-D-glucose	42.0 ± 3.4	156 ± 14	0.269	ND	ND	ND
D-Xylose	ND	ND	0.180	ND	ND	ND
1,5-Anhydro-D-glucitol	ND	ND	ND	20.7 ± 1.2	79.2 ± 5.3	0.261
Methyl β-D-glucoside	ND	ND	ND	35.2 ± 3.9	85.2 ± 12.4	0.413
Methyl α-D-glucoside	ND	ND	ND	20.1 ± 0.9	85.3 ± 5.1	0.236
Sophorose	ND	ND	ND	13.8 ± 1.1	49.8 ± 6.3	0.277
Laminaribiose	16.6 ± 1.4	156 ± 16	0.106	11.6 ± 1.0	29.1 ± 4.6	0.399
Cellobiose	ND	ND	ND	20.2 ± 0.7	22.2 ± 1.4	0.910
Gentiobiose	ND	ND	ND	26.1 ± 1.1	60.8 ± 4.4	0.429
Maltose	ND	ND	ND	5.07 ± 0.23	50.4 ± 3.5	0.101
N,N′-Diacetylchitobiose	ND	ND	ND	6.34 ± 0.15	49.9 ± 2.0	0.127
β-1,4-Mannobiose	ND	ND	ND	45.1 ± 1.1	30.7 ± 1.5	1.47
β-1,4-Mannotriose	ND	ND	ND	34.6 ± 0.3	13.3 ± 0.3	2.60
β-1,4-Mannotetraose	ND	ND	ND	31.2 ± 0.1	7.59 ± 0.16	4.11
β-1,4-Mannopentaose	ND	ND	ND	20.5 ± 0.3	5.29 ± 0.12	3.87
β-1,4-Mannohexaose	ND	ND	ND	16.0 ± 0.4	4.48 ± 0.26	3.57

[a] Reaction velocity at 40 mM.
[b] Reaction velocity was completely saturated at 0.05 mM, which is the lower limit of substrate concentration to determine accurate reaction velocity.

609.21, 771.27, 933.36, and 1095.37 m/z $[M + Na]^+$. These results indicate that rRaMP2 successively transferred mannosyl residues to the synthesized oligosaccharides. The chemical structures of the trisaccharides synthesized in the reactions in the presence of cellobiose and *N,N′*-diacetylchitobiose by rRaMP2 were analyzed as described above and determined to be 4-*O*-β-D-mannosyl-cellobiose and 4-*O*-β-D-mannosyl-*N,N′*-diacetylchitobiose, respectively (supplemental Table S1). ^{13}C and ^{1}H NMR spectra of the trisaccharides produced from β-1,4-mannobiose were completely identical to those of β-1,4-mannotriose.

Phosphorolysis of β-1,4-Mannooligosaccharides by rRaMP2—The kinetic analysis of the synthetic reaction of rRaMP2 indicated that this enzyme mainly catalyzes the phosphorolysis of β-1,4-mannooligosaccharides rather than that of Man-Glc. In the phosphorolytic reaction, rRaMP2 degraded β-1,4-mannotriose and β-1,4-mannotetraose to Man1*P* and shorter β-1,4-mannooligosaccharides (Fig. 4). β-1,4-Mannobiose was accumulated in the late stage of the reaction with β-1,4-mannotriose. The apparent kinetic parameters of rRaMP2 for Man-Glc and β-1,4-mannooligosaccharides, which were measured in the presence of 10 mM sodium phosphate buffer (pH 6.5), were compared (Table 4). The $k_{cat(app)}$ values for β-1,4-mannooligosaccharides longer than β-1,4- mannobiose were similar to that for Man-Glc, but the $K_{m(app)}$ values were 3.6–8.8-fold lower, consistent with the acceptor specificity for the synthetic reactions. On the other hand, β-1,4-mannobiose was a very poor substrate for rRaMP2. The $k_{cat(app)}/K_{m(app)}$ value was 22–65-fold lower than those for the longer β-1,4-mannooligosaccharides.

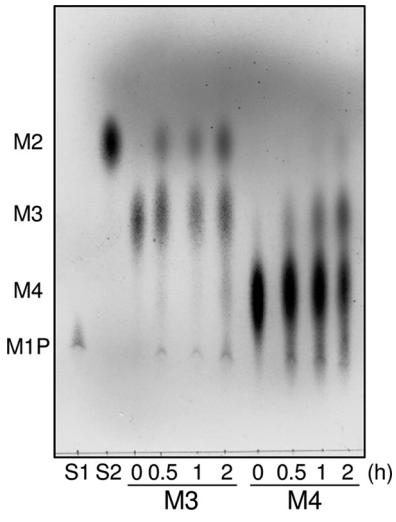

FIGURE 4. **Phosphorolysis of β-1,4-mannooligosaccharides by rRaMP2.** Phosphorolytic reactions of rRaMP2 toward β-1,4-mannotriose and β-1,4-mannotetraose were analyzed by TLC. Reaction time is indicated at the *bottom*. *S1* and *S2*, standards of Man1*P* and β-1,4-mannobiose, respectively. *M2*, β-1,4-mannobiose; *M3*, β-1,4-mannotriose; *M4*, β-1,4-mannotetraose; *M1P*, Man1*P*.

DISCUSSION

In *B. fragilis*, the metabolic pathway of mannan has been postulated as follows: (i) hydrolysis of mannan by extracellular β-1,4-mannanase, (ii) epimerization of the resulting β-1,4-mannobiose to Man-Glc by CE, and (iii) phosphorolysis of Man-Glc to D-glucose and Man1*P* by MP (7). Phosphomannose mutase and mannose-6-phosphate isomerase convert Man1*P* to fructose 6-phosphate, which is then metabolized through

TABLE 4

Apparent kinetic parameters for phosphorolysis of Man-Glc and β-1,4-mannooligosaccharides by rRaMP2

Kinetic parameters were calculated by fitting the initial velocities toward various concentrations of substrates in the presence of 10 mM inorganic phosphate to the Michaelis-Menten equation. Data are mean ± S.D. for three independent experiments.

	$k_{cat(app)}$	$K_{m(app)}$	$k_{cat(app)}/K_{m(app)}$	Relative $k_{cat(app)}/K_{m(app)}$
	s^{-1}	mM	s^{-1} mM^{-1}	*-fold*
Man-Glc	20.7 ± 0.7	28.4 ± 1.6	0.729	1
β-1,4-Mannobiose	7.06 ± 1.52	44.5 ± 11.0	0.159	0.218
β-1,4-Mannotriose	27.5 ± 6.1	7.94 ± 3.30	3.46	4.75
β-1,4-Mannotetraose	33.1 ± 10.3	3.21 ± 1.66	10.3	14.1
β-1,4-Mannopentaose	31.9 ± 12.4	4.55 ± 2.76	07.01	9.62

TABLE 5

Putative mannan-metabolizing enzymes of *R. albus* 7

Enzyme name	Locus	Localization	Homologous protein of *B. fragilis*
β-Mannanase	Rumal_0299, Rumal_0317, Rumal_0327, Rumal_0484, Rumal_0863, Rumal_1368, Rumal_2064, Rumal_3152	Extracellular	BF0764, BF0771
4-*O*-β-D-Mannosyl-D-glucose phosphorylase (RaMP1)	Rumal_0852	Intracellular	BF0772
β-1,4-Mannooligosaccharide phophorylase (RaMP2)	Rumal_0099	Intracellular	BF1316
Cellobiose 2-epimerase	Rumal_0019	Intracellular	BF0774
Phosphomannomutase	Rumal_2924	Intracellular	BF3668
Phosphomannose isomerase	Rumal_2865	Intracellular	BF1664
Sugar transport protein	Rumal_0598	Intracellular	BF0773

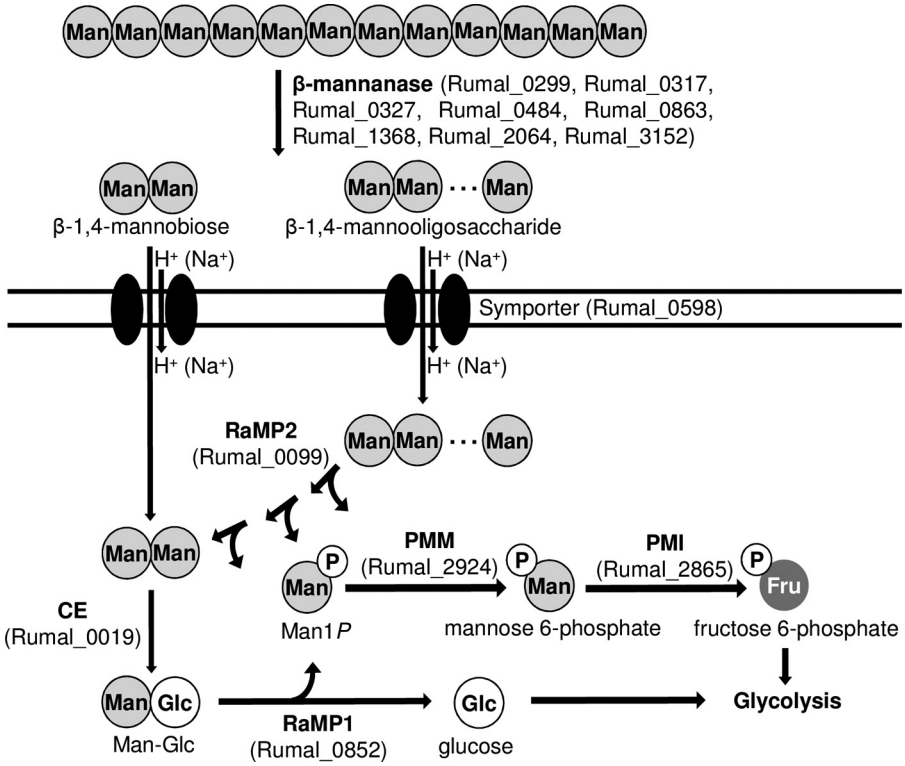

FIGURE 5. **Metabolic pathway of mannan in *R. albus* NE1.** The metabolic pathway of mannan involving two MPs and CE is illustrated. *PMM*, phosphomannose mutase; *PMI*, mannose 6-phosphate isomerase.

glycolysis. *R. albus* NE1 is also a CE producer (5), and two MP homologous genes were encoded in the genome of *R. albus* 7. This bacterium also has putative proteins involved in the metabolism of mannan, eight extracellular β-1,4-mannanases belonging to GH family 26, a phosphomannomutase, phosphomannose isomerase, and sugar transport protein similar to sugar/cation symporter (Table 5). MP activity was detected in the cell-free extract of *R. albus* NE1, and two MP isozymes, the deduced amino acid sequences of which are completely identical to the corresponding genes of *R. albus* 7, were found. Consequently, these MP isozymes are predicted to be physiologically functional, and *R. albus* NE1 (*R. albus* 7) is thought to degrade mannan through a similar pathway as postulated for *B. fragilis* (Fig. 5).

Both rRaMP1 and rRaMP2 catalyzed phosphorolytic and synthetic reactions of Man-Glc through a random Bi Bi mechanism in contrast to other known inverting carbohydrate phosphorylases (3, 32–34). Both rRaMP1 and rRaMP2 specifically catalyzed the phosphorolysis of a β-1,4-mannosidic linkage at the non-reducing end of a substrate, but they had acceptor specificities that were clearly different from each other. Consistent with the acceptor specificity of *B. fragilis* MP, which

shows high sequence similarity to RaMP1 (7), rRaMP1 was highly active only toward D-glucose and 6-deoxy-D-glucose, but rRaMP2 recognized a significantly wider variety of sugars, including oligosaccharides as the acceptor substrates. rRaMP2 was more active toward β-1,4-mannooligosaccharides than D-glucose, and successive formations of β-1,4-mannosidic linkages were observed in the synthetic reactions. In the phosphorolytic reactions, β-1,4-mannooligosaccharides were degraded to Man1*P* and shorter oligosaccharides (Fig. 4). β-1,4-Mannooligosaccharides longer than β-1,4- mannobiose were considerably better substrates for rRaMP2 than Man-Glc (Table 4). Hence, the physiological role of RaMP2 is not phosphorolysis of Man-Glc but is phosphorolysis of β-1,4-mannooligosaccharides of ≥DP3 to β-1,4-mannobiose. On the basis of the substrate preference, RaMP2 should be named β-1,4-mannooligosaccharide phosphorylase rather than 4-*O*-β-D-mannosyl-D-glucose phosphorylase. The low activity of rRaMP2 toward β-1,4-mannobiose clearly indicates the importance of the processes catalyzed by CE and RaMP1 as described above. *B. fragilis* also has a RaMP2-like protein, BF1316 (NCBI reference sequence, YP_210978.1), which has 64.6% sequence identity to RaMP2. It is possible that this bacterium also degrades mannooligosaccharides longer than β-1,4-mannobiose by the RaMP2-type phosphorylase. Furthermore, the aerobic CE-producing bacterium, *Rhodothermus murinus* (28), also has both RaMP1- and RaMP2-type proteins (YP_003291706 and YP_003291875, respectively), and hence, the metabolic pathway of mannan postulated here is not likely to be limited to anaerobic bacteria.

β-1,4-Mannotetraose was the best acceptor substrate for RaMP2 among the β-1,4-mannooligosacccharides tested in terms of the $k_{cat(app)}/K_{m(app)}$ (Table 3), whereas the $k_{cat(app)}/K_{m(app)}$ for longer β-1,4-mannooligosacccharides slightly decreased with an increase of DP. The acceptor site of RaMP2 is probably composed of at least four subsites. Hence, RaMP2 presumably has a cleft-type substrate binding site to accommodate a long chain acceptor substrate unlike RaMP1, which recognizes only monosaccharides as the acceptors. In the case of RaMP2, a β-1,4-glycosidic linkage is preferred in subsites +1 and +2, but the specificity for the acceptor substrates is very loose, and even maltose and *N*,*N*′-diacetylchitobiose were acceptable.

Herein, we described in detail the biochemical properties of two MP isozymes from *R. albus* NE1 belonging to GH family 130. Both enzymes were specific to the β-1,4-mannosidic linkage at the non-reducing end, but RaMP1 and RaMP2 showed narrow and broad acceptor specificities in synthetic reactions. RaMP2 is the first enzyme known to efficiently participate in the phosphorolysis and synthesis of β-1,4-mannooligosaccharides longer than β-1,4-mannobiose. Structural analysis of an enzyme-substrate complex is required for further understanding of the structure-function relationship of GH family 130 enzymes.

REFERENCES

1. Leatherwood, J. M. (1965) Cellulase from *Ruminococcus albus* and mixed rumen microorganisms. *Appl. Microbiol.* **13,** 771–775
2. Ohmiya, K., Shirai, M., Kurachi, Y., and Shimizu, S. (1985) Isolation and properties of β-glucosidase from *Ruminococcus albus*. *J. Bacteriol.* **161,** 432–434
3. Hamura, K., Saburi, W., Abe, S., Morimoto, N., Taguchi, H., Mori, H., and Matsui, H. (2012) Enzymatic characteristics of cellobiose phosphorylase from *Ruminococcus albus* NE1 and kinetic mechanism of unusual substrate inhibition in reverse phosphorolysis. *Biosci. Biotechnol. Biochem.* **76,** 812–818
4. Tyler, T. R., and Leatherwood, J. M. (1967) Epimerization of disaccharides by enzyme preparations from *Ruminococcus albus*. *Arch. Biochem. Biophys.* **119,** 363–367
5. Ito, S., Hamada, S., Yamaguchi, K., Umene, S., Ito, H., Matsui, H., Ozawa, T., Taguchi, H., Watanabe, J., Wasaki, J., and Ito, S. (2007) Cloning and sequencing of the cellobiose 2-epimerase gene from an obligatory anaerobe, *Ruminococcus albus*. *Biochem. Biophys. Res. Commun.* **360,** 640–645
6. Senoura, T., Taguchi, H., Ito, S., Hamada, S., Matsui, H., Fukiya, S., Yokota, A., Watanabe, J., Wasaki, J., and Ito, S. (2009) Identification of the cellobiose 2-epimerase gene in the genome of *Bacteroides fragilis* NCTC 9343. *Biosci. Biotechnol. Biochem.* **73,** 400–406
7. Senoura, T., Ito, S., Taguchi, H., Higa, M., Hamada, S., Matsui, H., Ozawa, T., Jin, S., Watanabe, J., Wasaki, J., and Ito, S. (2011) New microbial mannan catabolic pathway that involves a novel mannosylglucose phosphorylase. *Biochem. Biophys. Res. Commun.* **408,** 701–706
8. Hidaka, M., Kitaoka, M., Hayashi, K., Wakagi, T., Shoun, H., and Fushinobu, S. (2006) Structural dissection of the reaction mechanism of cellobiose phosphorylase. *Biochem. J.* **398,** 37–43
9. Cantarel, B. L., Coutinho, P. M., Rancurel, C., Bernard, T., Lombard, V., and Henrissat, B. (2009) The Carbohydrate-Active EnZymes database (CAZy). An expert resource for glycogenomics. *Nucleic Acids Res.* **37,** D233–D238
10. Egloff, M. P., Uppenberg, J., Haalck, L., and van Tilbeurgh, H. (2001) Crystal structure of maltose phosphorylase from *Lactobacillus brevis*. Unexpected evolutionary relationship with glucoamylases. *Structure* **9,** 689–697
11. Nagem, R. A., Rojas, A. L., Golubev, A. M., Korneeva, O. S., Eneyskaya, E. V., Kulminskaya, A. A., Neustroev, K. N., and Polikarpov, I. (2004) Crystal structure of exo-inulinase from *Aspergillus awamori*. The enzyme fold and structural determinants of substrate recognition. *J. Mol. Biol.* **344,** 471–480
12. Alberto, F., Bignon, C., Sulzenbacher, G., Henrissat, B., and Czjzek, M. (2004) The three-dimensional structure of invertase (β-fructosidase) from *Thermotoga maritima* reveals a bimodular arrangement and an evolutionary relationship between retaining and inverting glycosidases. *J. Biol. Chem.* **279,** 18903–18910
13. Nurizzo, D., Turkenburg, J. P., Charnock, S. J., Roberts, S. M., Dodson, E. J., McKie, V. A., Taylor, E. J., Gilbert, H. J., and Davies, G. J. (2002) *Cellvibrio japonicus* α-L-arabinanase 43A has a novel five-blade β-propeller fold. *Nat. Struct. Biol.* **9,** 665–668
14. Brüx, C., Ben-David, A., Shallom-Shezifi, D., Leon, M., Niefind, K., Shoham, G., Shoham, Y., and Schomburg, D. (2006) The structure of an inverting GH43 β-xylosidase from *Geobacillus stearothermophilus* with its substrate reveals the role of the three catalytic residues. *J. Mol. Biol.* **359,** 97–109
15. Fujimoto, Z., Ichinose, H., Maehara, T., Honda, M., Kitaoka, M., and Kaneko, S. (2010) Crystal structure of an exo-1,5-α-L-arabinofuranosidase from *Streptomyces avermitilis* provides insights into the mechanism of substrate discrimination between exo- and endo-type enzymes in glycoside hydrolase family 43. *J. Biol. Chem.* **285,** 34134–34143
16. Cartmell, A., McKee, L. S., Peña, M. J., Larsbrink, J., Brumer, H., Kaneko, S., Ichinose, H., Lewis, R. J., Viksø-Nielsen, A., Gilbert, H. J., and Marles-Wright, J. (2011) The structure and function of an arabinan-specific α-1,2-arabinofuranosidase identified from screening the activities of bacterial GH43 glycoside hydrolases. *J. Biol. Chem.* **286,** 15483–15495
17. Alhassid, A., Ben-David, A., Tabachnikov, O., Libster, D., Naveh, E., Zolotnitsky, G., Shoham, Y., and Shoham, G. (2009) Crystal structure of an inverting GH 43 1,5-α-L-arabinanase from *Geobacillus stearothermophilus* complexed with its substrate. *Biochem. J.* **422,** 73–82
18. Yamaguchi, A., Tada, T., Wada, K., Nakaniwa, T., Kitatani, T., Sogabe, Y., Takao, M., Sakai, T., and Nishimura, K. (2005) Structural basis for thermostability of endo-1,5-α-L-arabinanase from *Bacillus thermodenitrifi-*

cans TS-3. *J. Biochem.* **137,** 587–592
19. Meng, G., and Fütterer, K. (2003) Structural framework of fructosyl transfer in *Bacillus subtilis* levansucrase. *Nat. Struct. Biol.* **10,** 935–941
20. Martínez-Fleites, C., Ortíz-Lombardía, M., Pons, T., Tarbouriech, N., Taylor, E. J., Arrieta, J. G., Hernández, L., and Davies, G. J. (2005) Crystal structure of levansucrase from the Gram-negative bacterium *Gluconacetobacter diazotrophicus*. *Biochem. J.* **390,** 19–27
21. Sato, H., Saburi, W., Ojima, T., Taguchi, H., Mori, H., and Matsui, H. (2012) Immobilization of a thermostable cellobiose 2-epimerase from *Rhodothermus marinus* JCM9785 and continuous production of epilactose. *Biosci. Biotechnol. Biochem.* **76,** 1584–1587
22. Ito, S., Taguchi, H., Hamada, S., Kawauchi, S., Ito, H., Senoura, T., Watanabe, J., Nishimukai, M., Ito, S., and Matsui, H. (2008) Enzymatic properties of cellobiose 2-epimerase from *Ruminococcus albus* and the synthesis of rare oligosaccharides by the enzyme. *Appl. Microbiol. Biotechnol.* **79,** 433–441
23. Wakuta, S., Hamada, S., Ito, H., Matsuura, H., Nabeta, K., and Matsui, H. (2010) Identification of a β-glucosidase hydrolyzing tuberonic acid glucoside in rice (*Oryza sativa* L.). *Phytochemistry* **71,** 1280–1288
24. Moore, S., and Stein W. H. (1948) Photometric ninhydrin method for use in the chromatography of amino acids. *J. Biol. Chem.* **176,** 367–388
25. Miwa, I., Okudo, J., Maeda, K., and Okuda, G. (1972) Mutarotase effect on colorimetric determination of blood glucose with D-glucose oxidase. *Clin. Chim. Acta* **37,** 538–540
26. Cleland, W. W. (1963) The kinetics of enzyme-catalyzed reactions with two or more substrates or products. I. Nomenclature and rate equations. *Biochim. Biophys. Acta* **67,** 104–137
27. Lowry, O. H., and Lopez, J. A. (1946) The determination of inorganic phosphate in the presence of labile phosphate esters. *J. Biol. Chem.* **162,** 421–428
28. Ojima, T., Saburi, W., Sato, H., Yamamoto, T., Mori, H., and Matsui, H. (2011) Biochemical characterization of a thermophilic cellobiose 2-epimerase from a thermohalophilic bacterium, *Rhodothermus marinus* JCM9785. *Biosci. Biotechnol. Biochem.* **75,** 2162–2168
29. Rajashekhara, E., Kitaoka, M., Kim, Y.-K., and Hayashi, K. (2002) Characterization of a cellobiose phosphorylase from a hyperthermophilic eubacterium, *Thermotoga maritima* MSB8. *Biosci. Biotechnol. Biochem.* **66,** 2578–2586
30. Dixon, M., and Webb, E. C. (1979) *Enzymes*, 3rd Ed., pp. 109–110, Longman Group Ltd., London
31. Bock, K., and Pedersen, C. (1974) A study of ^{13}CH coupling constants in hexopyranoses. *J. Chem. Soc. Perkin Trans.* **2,** 293–297
32. Kitaoka, M., Sasaki, T., and Taniguchi, H. (1992) Phosphorolytic reaction of *Cellvibrio gilvus* cellobiose phosphorylase. *Biosci. Biotechnol. Biochem.* **56,** 652–655
33. Nihira, T., Nakai, H., Chiku, K., and Kitaoka, M. (2012) Discovery of nigerose phosphorylase from *Clostridium phytofermentans*. *Appl. Microbiol. Biotechnol.* **93,** 1513–1522
34. Kitaoka, M., Matsuoka, Y., Mori, K., Nishimoto, M., and Hayashi, K. (2012) Characterization of a bacterial laminaribiose phosphorylase. *Biosci. Biotechnol. Biochem.* **76,** 343–348